New Mexico Geological Society

Downloaded from: https://nmgs.nmt.edu/publications/guidebooks/76



Distributed Groundwater Recharge Quantification for the Sandia Basin, New Mexico: Orographic, Soil-Hydraulic, and DEM-Routed Infiltration Analysis

Todd Umstot, Kenny Calhoun, Farag Botros, and T. Neil Blandford
2026, pp. 409-420. https://doi.org/10.56577/FFC-76.409

in:

Geology of the Albuquerque Region - Fall Field Conference 2026, Connell, Sean D.; Koning, Daniel J.;, New Mexico Geological Society 76th Annual Fall Field Conference Guidebook, 452 p. https://doi.org/10.56577/FFC-76

This is one of many related papers that were included in the 2026 NMGS Fall Field Conference Guidebook.

Annual NMGS Fall Field Conference Guidebooks

Every fall since 1950, the New Mexico Geological Society (NMGS) has held an annual Fall Field Conference that explores some region of New Mexico (or surrounding states). Always well attended, these conferences provide a guidebook to participants. Besides detailed road logs, the guidebooks contain many well written, edited, and peer-reviewed geoscience papers. These books have set the national standard for geologic guidebooks and are an essential geologic reference for anyone working in or around New Mexico.

Free Downloads

NMGS has decided to make peer-reviewed papers from our Fall Field Conference guidebooks available for free download. This is in keeping with our mission of promoting interest, research, and cooperation regarding geology in New Mexico. However, guidebook sales represent a significant proportion of our operating budget. Therefore, only *research papers* are available for download. *Road logs*, *mini-papers*, and other selected content are available only in print for recent guidebooks.

Copyright Information

Publications of the New Mexico Geological Society, printed and electronic, are protected by the copyright laws of the United States. No material from the NMGS website, or printed and electronic publications, may be reprinted or redistributed without NMGS permission. Contact us for permission to reprint portions of any of our publications.

One printed copy of any materials from the NMGS website or our print and electronic publications may be made for individual use without our permission. Teachers and students may make unlimited copies for educational use. Any other use of these materials requires explicit permission.

This page is intentionally left blank to maintain order of facing pages.

New Mexico Geological Society Guidebook, 76th Fall Field Conference, 2026, p. 409–420, https://doi.org/10.56577/FFC-76.409

DISTRIBUTED GROUNDWATER RECHARGE QUANTIFICATION FOR THE SANDIA BASIN, NEW MEXICO: OROGRAPHIC, SOIL-HYDRAULIC, AND DEM-ROUTED INFILTRATION ANALYSIS

TODD UMSTOT[1], KENNY CALHOUN[1],
FARAG BOTROS[1], AND T. NEIL BLANDFORD[1]

[1]Daniel B. Stephens & Associates, Inc., 6501 Americas Parkway NE, Suite 200, Albuquerque, New Mexico 87110;
tumstot@geo-logic.com

Abstract—Groundwater recharge in the East Mountains region of Bernalillo County was quantified using the Distributed Parameter Watershed Model (DPWM), a bucket-type daily soil-water-balance framework derived from the MASSIF model developed for the proposed Yucca Mountain nuclear repository (Stein et al., 2007). The model domain includes the eastern slope of the Sandia Mountains as well as South Mountain and San Pedro Mountain. The model incorporates the communities of Cedar Crest, Sandia Park, Golden, Placitas, and the northern portion of Tijeras.

The daily water balance was simulated for water years 1971 through 2015. Actual evapotranspiration was computed using the FAO-56 Penman-Monteith method with vegetation data from United States Geological Survey (USGS) GAP maps and National Aeronautics and Space Administration (NASA) Moderate Resolution Imaging Spectroradiometer (MODIS) satellite imagery, soil hydraulic parameters from U.S. Department of Agriculture (USDA) soil maps with van Genuchten retention curves estimated via the Rosetta pedotransfer method, and a bedrock boundary that constrains drainage where saturated hydraulic conductivity falls below the infiltration rate.

The majority of simulated recharge occurs at higher elevations in the Sandia Mountains and along washes crossing relatively flat areas at lower elevations. Negligible diffuse recharge was estimated between the washes. Over the entire DPWM domain, mean annual recharge is approximately 15×10^6 m^3/yr, which represents about 4% of average precipitation. The percentage ranges from 1.2% to 9.0% on an annual basis over the simulation period. This is a lower bound estimate compared to other studies of recharge in the East Mountains. DPWM simulations account for climate trends in precipitation and air temperature that may affect snow pack and recharge. We found that recharge in recent decades is not consistently higher or lower compared to earlier decades. DPWM could be used with scaled climate models to predict groundwater recharge under changing climate conditions

INTRODUCTION

Recharge is atmospheric water that reaches the regional water table. Recharge is the most significant water balance input to the East Mountains aquifer system; there are no perennial surface water bodies, rivers, or substantial lateral inflows from adjoining basins to contribute to groundwater within the study area (Bartolino et al., 2010). Recharge potential depends on precipitation amount and duration, surficial and bedrock geology, soil depth and permeability, land surface slope and orientation, and vegetation type. Although potential evapotranspiration may exceed precipitation annually, during winter, early spring, or intense summer storms, evapotranspiration can be less than precipitation, and it is at these times where the potential for recharge is greatest.

For recharge to occur, precipitation must pass through the soil column rapidly or it will be removed through evapotranspiration. This requires that infiltrating water exceed both the evapotranspiration rate and soil storage capacity. In the East Mountains climate, this occurs through focused recharge (water collection in depressions or stream channels) or broad recharge on thin mountain soils. Four categories of recharge occur:

- Mountain block recharge: In mountainous terrain with exposed bedrock, minimal or absent soil limits moisture storage and vegetation, resulting in low evapotranspiration. Infiltration potential is highest where bedrock is permeable. The greatest recharge typically occurs at higher elevations where precipitation is greater, soils are thinner, and bedrock is permeable (Wilson and Guan, 2004).
- Mountain front recharge: Precipitation runoff from mountain terrain flows through ephemeral washes and recharges in the transition zone between mountain block and valley floor (Wilson and Guan, 2004). Washes collect runoff from the mountain block. This rapid recharge reaches the water table within days to months (McCoy and Blanchard, 2008).
- Local recharge: Focused infiltration and deep percolation occur in locations such as unvegetated sandy drainages or temporary areas of ponding. Infrequent storms can generate recharge at these sites (Stewart-Deaker et al., 2007). This rapid recharge reaches the water table within days to months (McCoy and Blanchard, 2008).
- Diffuse recharge: Precipitation infiltrating broad lowland areas between washes percolates through surficial soils and is stored as soil moisture. Most of this water is removed by evapotranspiration. Water not removed may migrate toward the water table, particularly at higher valley elevations or where deep fissures or macropores exist. Diffuse recharge is generally minimal in desert

basins and slow, reaching the water table over years to decades. Current diffuse recharge likely originated from precipitation decades or more ago (Phillips, 1994).

The study area encompasses the eastern slopes of the Sandia Mountains, bounded by Sandia Crest to the west, South Mountain to the east, Interstate 40 to the south, and several miles north of Hagan to the north (Fig. 1). Soils are generally thin, with many bedrock exposures, except in lower-elevation areas adjoining San Pedro Creek and the northern portion of the study area in the Hagan Basin, where unconsolidated sediments thicken. The ground surface elevation ranges from 1,585 m above mean sea level (msl) to 3,231 m msl; mean elevation is 2,073 m msl.

The primary surface drainage in the study area is San Pedro Creek, which headwaters in the Sandia Mountains and runs eastward downslope until it passes San Antonito and is joined by the smaller Frost Arroyo, after which it runs north to eventually join the Rio Grande. Except where springs are present, surface drainages in the East Mountains are dry for the majority of the year and flow only in response to rapid rainfall or snowmelt. A surface water divide is present in the study area in the hills south of Frost Road; surface water north of the divide flows to the Rio Grande through the Hagan or Placitas areas, and surface water south of the divide flows to the Rio Grande through Tijeras Arroyo (Bartolino et al., 2010). When flow occurs, these channels are losing reaches where streamflow infiltrates through alluvial streambed sediments and recharges the underlying aquifer, representing an important pathway for mountain front recharge (Wilson and Guan, 2004).

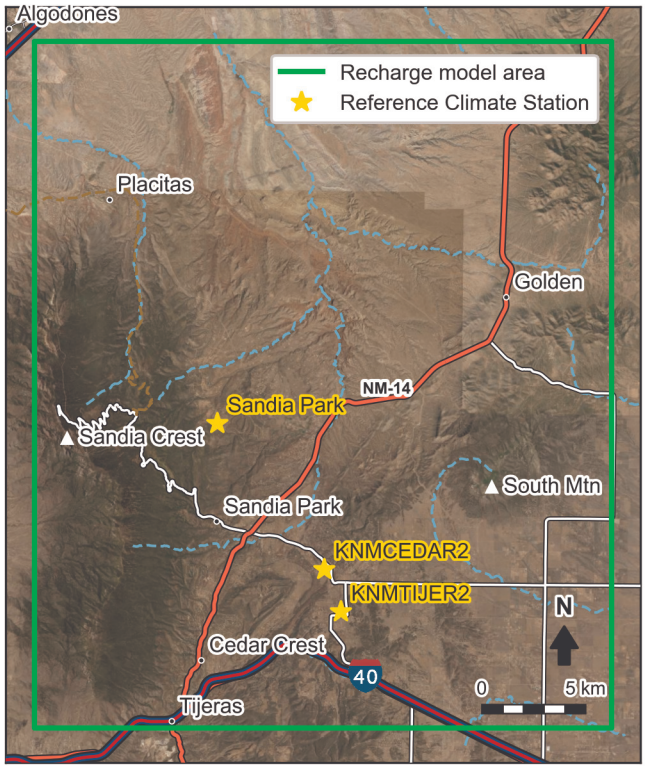


FIGURE 1. Location and physiography of the East Mountains.

Prior Studies

Few studies provide groundwater recharge estimates for the East Mountains that are not based on simple precipitation percentages using transfer equations (e.g., Maxey and Eakin, 1949). Bartolino et al. (2010) reviewed East Mountains recharge studies based primarily on transfer equations and developed recharge ranges for several watersheds. For the San Pedro Creek watershed, they estimated recharge of 0.5×10^6 to 9.5×10^6 m³/yr (385 to 7,700 acre-ft/yr), or 0.5% to 10% of mean annual precipitation. While useful for preliminary estimates, transfer equation methods do not account for basin-specific climate, soil, vegetation, and bedrock properties (D'Agnese et al., 1997).

The USGS has published three reports with recharge or evapotranspiration estimates independent of transfer equations: McCoy and Blanchard (2008), Rice and Crilley (2014), and Douglas-Mankin et al. (2020).

McCoy and Blanchard (2008) and Rice and Crilley (2014) used chloride mass balance methods with precipitation and spring measurements to estimate recharge to the Madera Formation above 2,286 m elevation in the Sandia Mountains. McCoy and Blanchard (2008) estimated recharge to the 34-km² area ranged from 1.2×10^6 to 4.3×10^6 m³/yr (1,000 to 3,500 ac-ft/yr), or 7% to 23% of mean precipitation. Rice and Crilley (2014), who included chloride measurements from lower-elevation springs in the Abo Formation, found similar rates: 5.5% to 23% of annual precipitation.

Douglas-Mankin et al. (2020) conducted a 1-year study evaluating evapotranspiration and available water across the East Mountains area using PRISM precipitation data and satellite-based Operational Simplified Surface Energy Balance (SSEBop) model estimates at 100-m resolution. In 2015, precipitation was 608 mm while actual evapotranspiration was 543 mm (89%), leaving approximately 65 mm of available water. The study did not partition available water among runoff, storage, and recharge, and the SSEBop method does not account for snow sublimation as a separate loss term.

METHODOLOGY

We applied the DPWM to develop an independent estimate of recharge for a groundwater flow model in support of a water rights application filed with the New Mexico Office of the State Engineer in the East Mountains portion of the Sandia Basin. The DPWM performs a detailed daily water mass balance over a fine spatial discretization, tracking the quantity of water passing through the root zone as net infiltration. The recharge model area is rectangular, extending 27.4 km east–west and 33.8 km north–south and covering 920 km² (Fig. 1).

The DPWM was developed by Daniel B. Stephens & Associates, Inc. based on the Mass Accounting System for Soil Infiltration and Flow (MASSIF) model developed by Sandia National Laboratories (Stein et al., 2007) for the Yucca Mountain Project. The DPWM is similar in concept to water balance models used by the USGS (e.g., PRMS [Leavesley et al., 1983], INFIL [Hevesi et al., 2003], BCM [Flint and Flint, 2007]). The

DPWM operates on a daily time step with a spatial resolution of 8,361 m² (91.4 m × 91.4 m) grid cells. Water budget components include precipitation, bare soil evaporation, transpiration, runoff, run on, snow accumulation, snowmelt, snow sublimation, soil water storage, and net infiltration. Actual evapotranspiration is computed from reference evapotranspiration using the FAO 56 Penman-Monteith methodology with phenology-scaled basal crop coefficients modulated by water stress, bare-soil evaporative reduction, and dynamic canopy fractions. A bedrock boundary is placed at the bottom of DPWM cells with shallow soil depths; this boundary restricts infiltration when the saturated hydraulic conductivity of the bedrock is less than that of the soil.

Input Data

Model input data were obtained from weather stations, published literature, and related property estimates. Where data were unavailable or uncertain, parameter values were conservatively selected to underestimate recharge.

Climate

The highest elevations of the East Mountains area are classified as subhumid/humid in climate, and the lower elevations are classified as semiarid (Bartolino et al., 2010), though no distinct elevation threshold separates the two climate zones. The average annual precipitation as predicted from the PRISM precipitation maps (Daly et al., 1994) for the period 1981 through 2010 ranges from 279 to 686 mm. Most of the annual precipitation occurs as snowfall from January through March and as monsoonal rainfall from July through September, with the summer monsoon accounting for nearly half of annual precipitation (McCoy and Blanchard, 2008; Julyan and Stuever, 2005; Douglas-Mankin et al., 2020). Annual snowpack can exceed 2,540 mm at Sandia Crest (Julyan and Stuever, 2005). At the National Oceanic and Atmospheric Administration (NOAA) Sandia Park weather station at 2,143 m elevation, snowfall averaged 1,510 mm/yr from 1981 through 2010 (Douglas-Mankin et al., 2020).

Direct climate inputs to the DPWM include daily total precipitation, maximum and minimum air temperature, and average wind speed. Climate data were obtained from the NOAA Sandia Park meteorological station (Fig. 1). Precipitation data gaps were filled using daily PRISM predictions for the station location. Figure 2 shows total annual precipitation for the simulation period (water years 1971–2015).

The spatial distribution of precipitation across the model domain was derived from the PRISM 1981–2010 mean annual precipitation normals (Daly et al., 1994). PRISM climatological normals are 30-year average precipitation datasets published each decade by the PRISM Climate Group at Oregon State University. The normals map was used solely as a static spatial weighting function to distribute observed daily precipitation from the Sandia Park station across model grid cells. Figure 3 depicts the distribution of mean annual precipitation estimated by DPWM from the PRISM normals map and the Sandia Park station over the simulation period.

Each daily time step with precipitation is divided into two phases: (1) the precipitation event duration and (2) the remainder of the day. Precipitation duration is assumed to be 6 hours, except 2 hours during July–September monsoon storms and 12 hours for snowmelt days. Storm duration controls the effective infiltration capacity of soil and bedrock where shorter

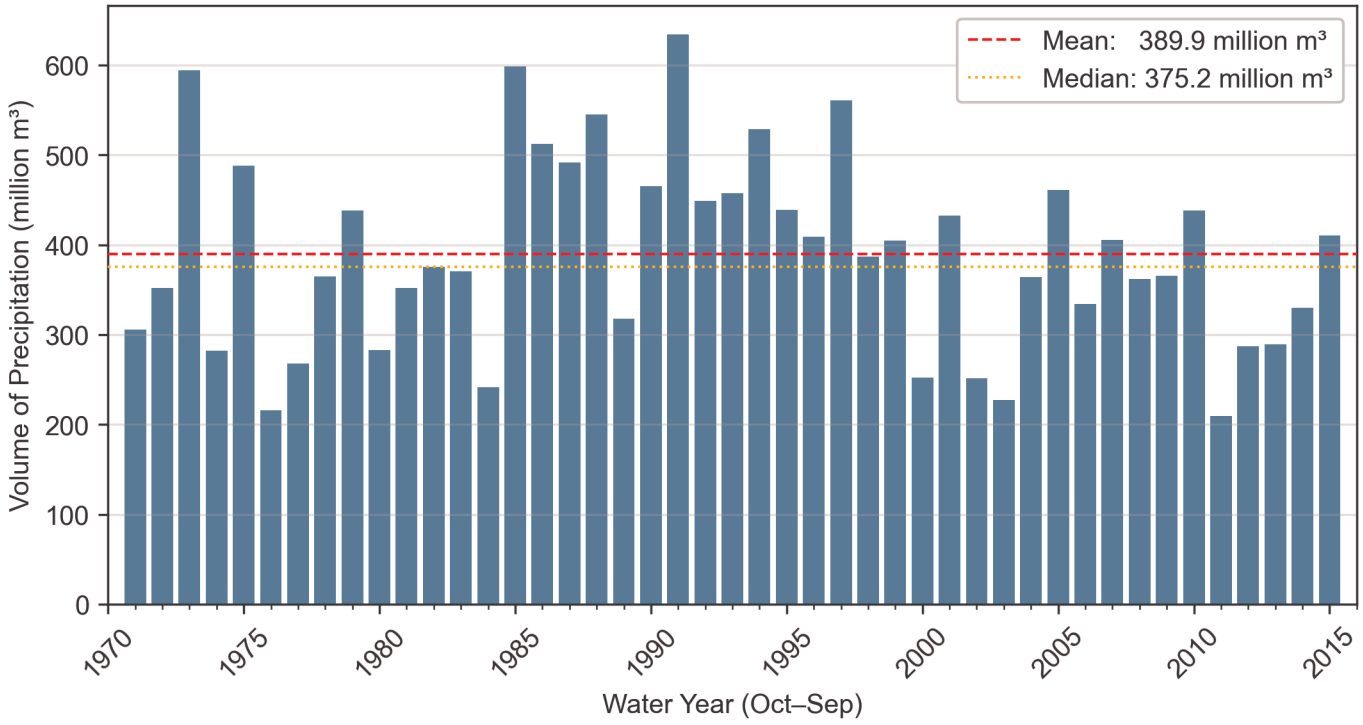


FIGURE 2. Plot of total annual precipitation within the DPWM model domain for water years 1971 to 2015.

durations concentrate the same precipitation volume into a higher intensity, increasing runoff and reducing infiltration. The 2-hour monsoon duration reflects the characteristically brief, high-intensity convective storms of the monsoon season, while the 6-hour winter duration reflects the longer, lower-intensity frontal precipitation typical of the region. A Latin hypercube sensitivity analysis of the DPWM conducted for the Tule Desert basin in Nevada (Daniel B. Stephens & Associates, Inc., 2009) found that precipitation intensity, which is inversely related to storm duration, was not a significant contributor to uncertainty in mean annual net infiltration, whereas precipitation amount and soil depth were the dominant controls. This suggests that the specific duration assumptions used here have limited influence on the overall recharge estimate relative to other model parameters, though they may influence the partitioning between runoff and infiltration at the cell scale.

Precipitation falls as snow when daily average temperature is below 32°F. Because air temperature varies with elevation across the model domain, both rain and snow may occur on a given day. Snow is stored as water-equivalent depth and sublimates daily at the reference evapotranspiration rate using an albedo of 0.60, following INFIL model methodology (USGS, 2008).

When snowpack is present and temperature exceeds 32°F, snow melts at seasonally varying rates ranging from 2.0 mm/d/°C (December 21) to 5.2 mm/d/°C (June 21) using a temperature-index approach based on the HELP model SNOW-17 routine (Schroeder et al., 1994), which serves as an empirical surrogate for the full surface energy balance. The temperature-index method is well established for regional-scale water balance modeling where distributed radiation data are unavailable (Wilson and Guan, 2004), although it does not explicitly resolve radiation, turbulent heat fluxes, or albedo dynamics, and it may underestimate early-season melt on south-facing slopes and overestimate melt under warm, cloudy conditions with low net radiation.

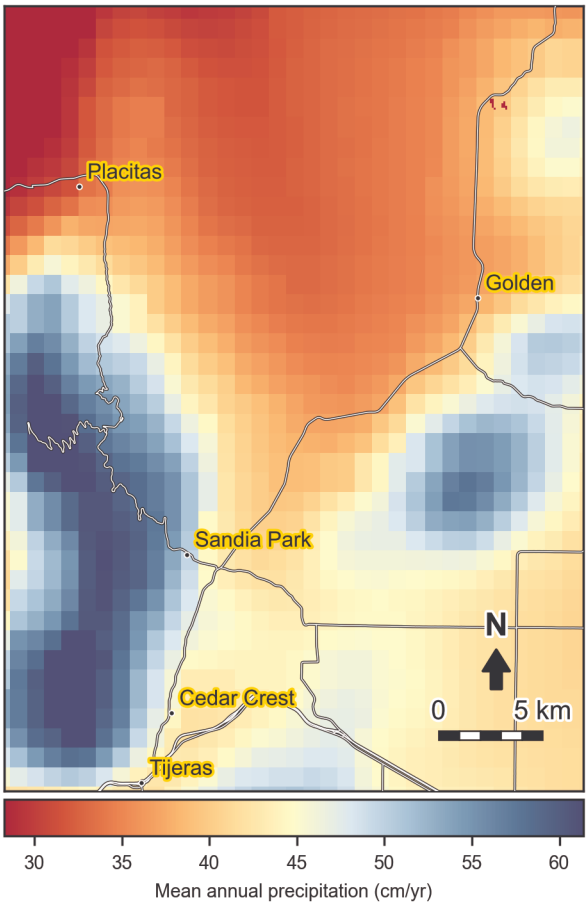


FIGURE 3. Map of mean annual precipitation simulated by DPWM.

Air temperature data from Sandia Park were lapse-corrected for elevation (-7.0°C/km) using mean annual maximum temperatures from PRISM 1971–2000 normals. Missing temperature data were supplemented with daily PRISM data.

Wind speed data from Albuquerque Sunport were adjusted by +1.41 m/s based on average differences with East Mountains stations available on Weather Underground (ABQ-KNMTIJER2 and ABQ-KNMCEDAR2) over the period from October 2009 through December 2015. Estimated wind speeds below 0.5 m/s were set to 0.5 m/s per FAO-56 recommendations (Allen et al., 1998).

Soils

Soil data were obtained from the USDA Soil Survey Geographic database (SSURGO; Soil Survey Staff, 2010), based on field surveys conducted in the East Mountains. The SSURGO database provides texture (percent sand, silt, clay), saturated hydraulic conductivity, dry bulk density, saturated water content, and water contents at 1/3 and 15 bars for each soil horizon. The dominant soil component by area was assigned to each map unit, and weighted-average properties were computed based on layer thicknesses. Water retention characteristics were estimated using the Rosetta pedotransfer method (Schaap et al., 2001) with texture data, water contents, and bulk densities from SSURGO. For soils shallower than 2 m, USDA depth ranges were used. Where SSURGO records did not specify soil depth (i.e., soils thicker than 2 m), total soil column depth was set to 20 m. The rooting zone remains 2 m regardless of total soil depth; the additional 18 m represents unsaturated storage between the base of the root zone and the bedrock boundary. Sensitivity simulations on the maximum 20-m thickness showed negligible effect on simulated recharge rates or evapotranspiration.

Field capacity was set to 1/10 bar (102 cm), the upper end of the typical 1/3 to 1/10 bar range (Stein et al., 2007), and wilting point was set to 60 bar (61,293 cm), above the typical 15 bar value. Together, these values define a wider plant-available water range than typically assumed, which decreases infiltration and increases water availability for evapotranspiration. This wider range also accounts for layered soil heterogeneity not explicitly resolved by the DPWM, which can impede infiltration and increase evapotranspiration relative to homogeneous soil assumptions. Desert vegetation can tolerate wilting points up to 60 bars (Stein et al., 2007).

Figure 4 shows the available soil water (ASW) in the root zone. ASW across the DPWM domain ranges from zero in bare

rock outcrop areas to a maximum of 53 cm, with a domain-wide mean of 20.6 cm and median of 15.0 cm. Rock outcrop soils, which hold negligible plant-available water due to their low water retention properties, account for approximately 2.6% of the domain. Among cells with soil cover, approximately 35% have ASW below 10 cm, 23% between 10 and 20 cm, 10% between 20 and 30 cm, and 30% exceeding 30 cm,

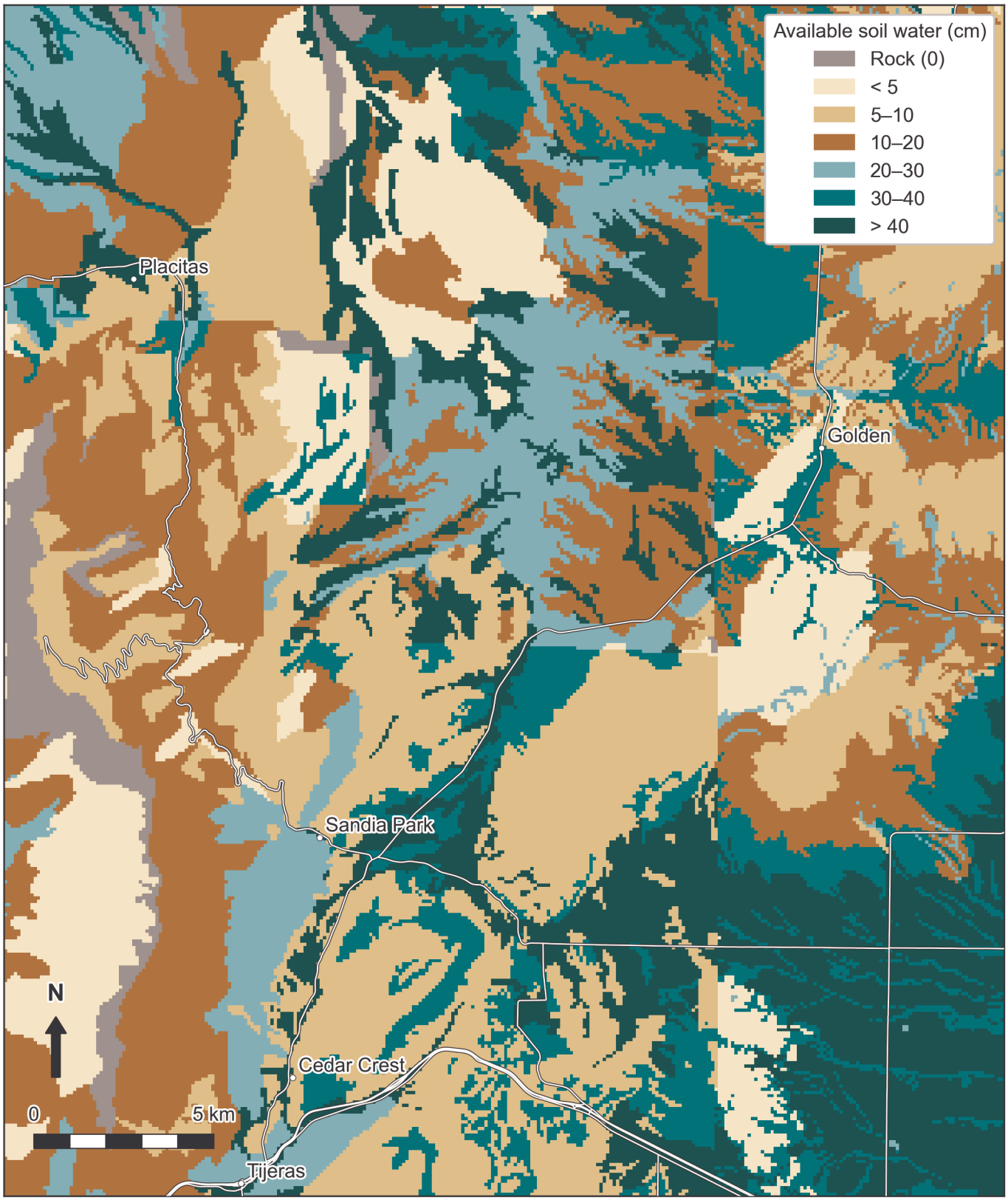


FIGURE 4. Map of available soil water (ASW) in DPWM.

with the highest values corresponding to deep, fine-textured soils at lower elevations where soil development is greatest.

Bedrock

The bedrock geology of the East Mountains consists primarily of layered sedimentary rocks, including limestone, sandstone, and shale, that have been folded and faulted into complex structures. These sedimentary layers overlie relatively impermeable Precambrian granite. From oldest to youngest, the sedimentary sequence includes the Pennsylvanian Madera Formation (limestone), the Permian Abo and Yeso Formations (sandstone and mudstone), and younger layers such as the Triassic Chinle Group (shale and sandstone), the Jurassic Morrison Formation (sandstone and mudstone), and a thick Cretaceous sequence comprising the Dakota Sandstone, Mancos Shale, and Mesaverde Group (Williams and Cole, 2007; Bartolino et al., 2010).

Bedrock underlying the soils of the study area may restrict net infiltration when the saturated hydraulic conductivity of the bedrock is less than the infiltration rate and soil thickness is limited. The distribution of bedrock types was obtained from the Williams and Cole (2007) geologic map. Saturated vertical hydraulic conductivities were obtained from a calibrated groundwater flow model within the DPWM domain (Table 1). The DPWM bedrock vertical hydraulic conductivities were updated iteratively as the groundwater model was refined.

The minimum of soil and bedrock saturated hydraulic conductivity (called limiting hydraulic conductivity) controls the maximum rate of infiltration through the soil-bedrock column (Fig. 5). Across the DPWM domain, limiting hydraulic conductivity ranges over four orders of magnitude from approximately 1.3×10^{-4} to 2.54 cm/hr. The median value of 0.064 cm/hr reflects the dominance of low-permeability sediment across much of the model domain. Approximately 25% of model cells have limiting conductivities exceeding 1 cm/hr, corresponding to areas underlain by Quaternary alluvium or mapped as bare rock with high soil hydraulic conductivity. In these areas, recharge is not limited by vertical hydraulic conductivity and is controlled by other factors such as precipitation intensity and soil storage. In contrast, cells with the lowest limiting conductivities (below 0.001 cm/hr) effectively limit recharge regardless of surface water availability.

Vegetation

Vegetation across the model domain ranges from desert scrub at the lowest elevations to conifer forest on the upper Sandia Mountains block, with piñon-juniper woodland covering the majority of the domain. Vegetation type distribution was obtained from digital land cover datasets provided by the Southwest Gap land cover mapping project (USGS, 2026; Lowry et al., 2005). Leaf area index (LAI), the ratio of one-sided leaf area to total land area (m^2/m^2), indicates vegetation density. Monthly LAI values were obtained from NASA MODIS satellite datasets (USGS, 2010) for water year 2005 (October 2004 through September 2005), an above-average precipitation year. The MODIS LAI pattern was also used to define monthly phenology for each vegetation association, including leaf initiation, peak growing season, growth decline, and dormancy. These data represent measurements of actual vegetation within the East Mountains.

Using a single above-average-year LAI as a static input likely overestimates evapotranspiration and underestimates recharge by a modest amount. This effect is constrained, however, by the dominance of piñon-juniper woodland and evergreen forest across the model domain. These perennial, drought-tolerant species exhibit relatively stable LAI between wet and dry years compared to annual or deciduous vegetation.

Topography

Topography data serve two primary functions in the DPWM: routing surface flow and adjusting incoming solar radiation based on land surface slope and aspect. Model topography was derived by averaging USGS 10-m resolution digital elevation models (DEMs) to the DPWM grid resolution of 91.4 m, retaining average slope, azimuth, and elevation values for each grid cell. Topography influences DPWM reference evapotranspiration calculations through terrain-adjusted solar radiation estimates (Allen et al., 2006). The translation procedure for slope and azimuth follows the methods published by Reindl et al. (1990) and Duffie and Beckman (1980, 1991).

TABLE 1. Saturated vertical hydraulic conductivity of geologic units used in the DPWM

Formation code	Formation age and name	K (m/s)	Permeability class
Qa	Quaternary alluvium	7.06×10^{-6}	high
Kv	Cretaceous Mesaverde Group	3.53×10^{-8}	low
Km	Cretaceous Mancos Shale	3.53×10^{-10}	very low
Kd	Cretaceous Dakota Sandstone	3.53×10^{-8}	low
Jm	Jurassic Morrison Formation	3.53×10^{-9}	very low
Jb	Jurassic undifferentiated	3.53×10^{-9}	very low
Trc	Triassic Chinle	5.20×10^{-10}	very low
Trm	Triassic Moenkopi	4.23×10^{-7}	moderate
Trz	Triassic Agua Zarca / Santa Rosa Sandstone	1.76×10^{-8}	low
Psg	Permian San Andres / Glorieta Sandstone	1.71×10^{-6}	moderate–high
Py	Permian Yeso Formation	3.42×10^{-7}	moderate
Pa	Permian Abo Formation	2.99×10^{-9}	very low
Pm	Pennsylvanian Madera Formation	1.46×10^{-8}	low
Ps	Pennsylvanian Sandia Formation	7.06×10^{-8}	low
PreC	Precambrian granite / metamorphic	3.53×10^{-10}	very low
Ti	Tertiary intrusive	1.76×10^{-7}	low–moderate

Although the DEM is aggregated to the model grid resolution for evapotranspiration calculations, channel definition in the DPWM does not rely solely on the aggregated DEM. Wash locations were identified using both mapped wash locations and DEM-derived flow accumulation, and each grid cell intersecting a wash was divided into a wash subcell and an interwash subcell with distinct soil hydraulic properties. Wash widths were assigned as a function of upstream flow

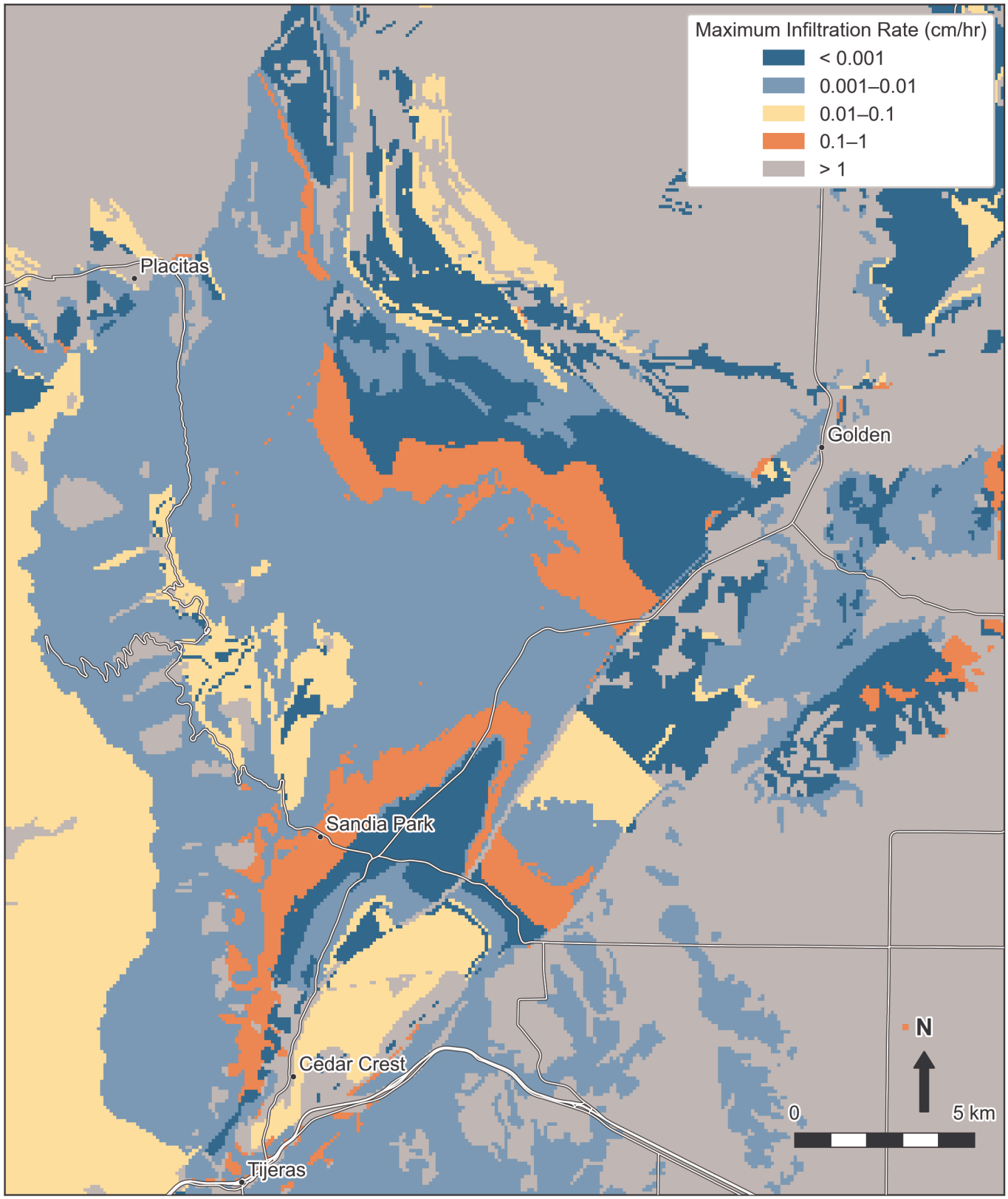


FIGURE 5. Map of infiltration capacity in DPWM.

accumulation, ranging from 1 to 10 m. Runoff from interwash subcells is routed to the wash subcell within each grid cell, and wash outflow is passed downstream based on DEM-derived flow direction.

RESULTS AND DISCUSSION

Water balance components were determined for water years 1971–2015; mean values are provided in Table 2. Mean annual recharge distribution is shown in Figure 6. Most simulated recharge occurs at higher elevations in the Sandia Mountains and in washes crossing lower-elevation flat areas. Negligible diffuse natural recharge is simulated between washes, consistent with previous studies (e.g., Phillips, 1994). Mean precipitation for the entire DPWM domain is approximately 390×10^6 m^3/yr (Fig. 3), with simulated mean net recharge of 15×10^6 m^3/yr (about 4% of precipitation). This is a lower bound estimate of recharge compared to other studies in the East Mountains, as discussed below.

The DPWM simulates each of the recharge pathways through its gridded daily water balance structure. Mountain block recharge is represented by recharge computed at upland cells where thin soils and permeable bedrock allow drainage below the root zone. Mountain front and local recharge are captured through the model's explicit runoff routing network, in which saturation-excess runoff is routed as run-on to downstream cells; cells intersecting washes are subdivided into a high-permeability wash cell and an adjacent interwash cell, concentrating infiltration where channelized flow is received. Diffuse recharge is computed at every interwash cell but typically yields zero recharge where root zones are thick under the simulated East Mountains climate conditions. This is a structural outcome of the soil water balance using the field capacity method rather than a prescribed assumption and is consistent with previous findings of negligible diffuse recharge in semiarid basins (e.g., Phillips, 1994). The DPWM output reported in this paper is net infiltration, which is the water draining below the root zone and is used as a proxy for groundwater recharge. Travel time from below the root zone to the water table is not simulated.

Recharge as a percentage of precipitation varied from 1.2% to 9.0% (median 2.8%) across the 45 simulated water years. Except for the dry water year 1990, the period 1985–1995 had notably higher recharge, while the periods 1979–1984 and 2011–2015 had relatively lower recharge (Fig. 7). To assess whether these decadal patterns reflect a systematic long-term trend, Mann-Kendall trend tests were applied to both the annual recharge and annual precipitation time series. For annual recharge, the Mann-Kendall test yielded a Tau of -0.014 and a Sen slope of -6.8 acre-ft/yr ($p = 0.90$), indicating a negligible and statistically insignificant downward tendency. For annual precipitation, the Sen slope was -1,088 acre-ft/yr ($p = 0.43$), also not significant. Neither result exceeds the $\alpha = 0.05$ significance threshold. The apparent decadal variability therefore reflects natural multiyear climate oscillations rather than a directional change in the hydrologic system, consistent with the episodic and climatically driven nature of recharge in semiarid mountain environments.

Analysis of the relationship between ASW and simulated recharge reveals a strong and statistically significant inverse relationship. The Spearman rank correlation between ASW and recharge is -0.69 ($p < 0.001$), indicating that cells with higher water-holding capacity consistently generate less recharge. This pattern is most pronounced when comparing recharge and no-recharge cells directly: cells that generate recharge have a mean ASW of 10.8 cm (median 8.7 cm), while cells with no simulated recharge have a mean ASW of 34.0 cm (median 36.7 cm). The relationship is nonlinear and threshold-like rather than gradual. Cells with ASW below 10 cm show the highest mean recharge rates (2.21–2.54 cm/yr) and the greatest frequency of recharge occurrence (88% to 92% of cells), whereas cells with ASW exceeding 20 cm show dramatically lower mean recharge rates (below 0.23 cm/yr) and recharge occurrence drops sharply to less than 20% of cells.

Simulated recharge increases strongly and significantly with elevation across the DPWM domain. The Spearman rank correlation between elevation and recharge is 0.45 ($p < 0.001$), and a Mann-Kendall trend test on elevation-binned mean recharge gives a statistically significant monotonic increase with elevation (Tau = 0.78, $p = 0.005$). At the lowest elevations (1,500–1,700 m), mean annual recharge is approximately 1.7 cm/yr, representing 6% of precipitation, with only 27% of cells generating any recharge; the elevated recharge percentage in this band relative to mid-elevations reflects the concentration of recharge in wash cells within a small cell population. Recharge rates are lowest in the broad mid-elevation zone between 1,700 and 2,100 m, where mean annual recharge is approximately 0.6 cm/yr and represents only 1.6% to 2.0% of precipitation, with 38% to 55% of cells generating recharge. Rates increase progressively above 2,100 m: the 2,100–2,300 m band averages 1.6 cm/yr (3.4% of precipitation, 72% recharge occurrence), rising to 2.6 cm/yr (4.9% of precipitation, 84% recharge occurrence) in the 2,300–2,500 m band. Above 2,500 m, recharge occurrence reaches 93% to 100% of cells and mean annual rates range from 4.6 cm/yr in the 2,500–2,700 m band to 18.7 cm/yr above 3,100 m, representing 8% to 30% of precipitation. Despite comprising only 8% of the model domain by cell count, the high-elevation Sandia Mountain block generates large recharge volumes; cells above 2,500 m recharge at mean rates approximately 7.5 times higher than cells below 2,500 m,

TABLE 2. Mean annual water balance components

Precipitation (m^3/yr)	Actual evapotranspiration (m^3/yr)	Recharge (m^3/yr)	Runoff out of model domain (m^3/yr)	Change in soil-water storage (m^3/yr)	Change in snowpack (m^3/yr)	Sublimation (m^3/yr)
389,920,000	284,960,000	14,720,000	7,180,000	480,000	—	82,580,000

consistent with the orographic precipitation gradient and the prevalence of shallow, rocky soils at high elevations that limit evapotranspiration and increase deep percolation.

Model results were evaluated against independent USGS recharge estimates for overlapping subareas of the study domain (McCoy and Blanchard, 2008; Bartolino et al., 2010; Rice and Crilley, 2014). These USGS estimates are based on

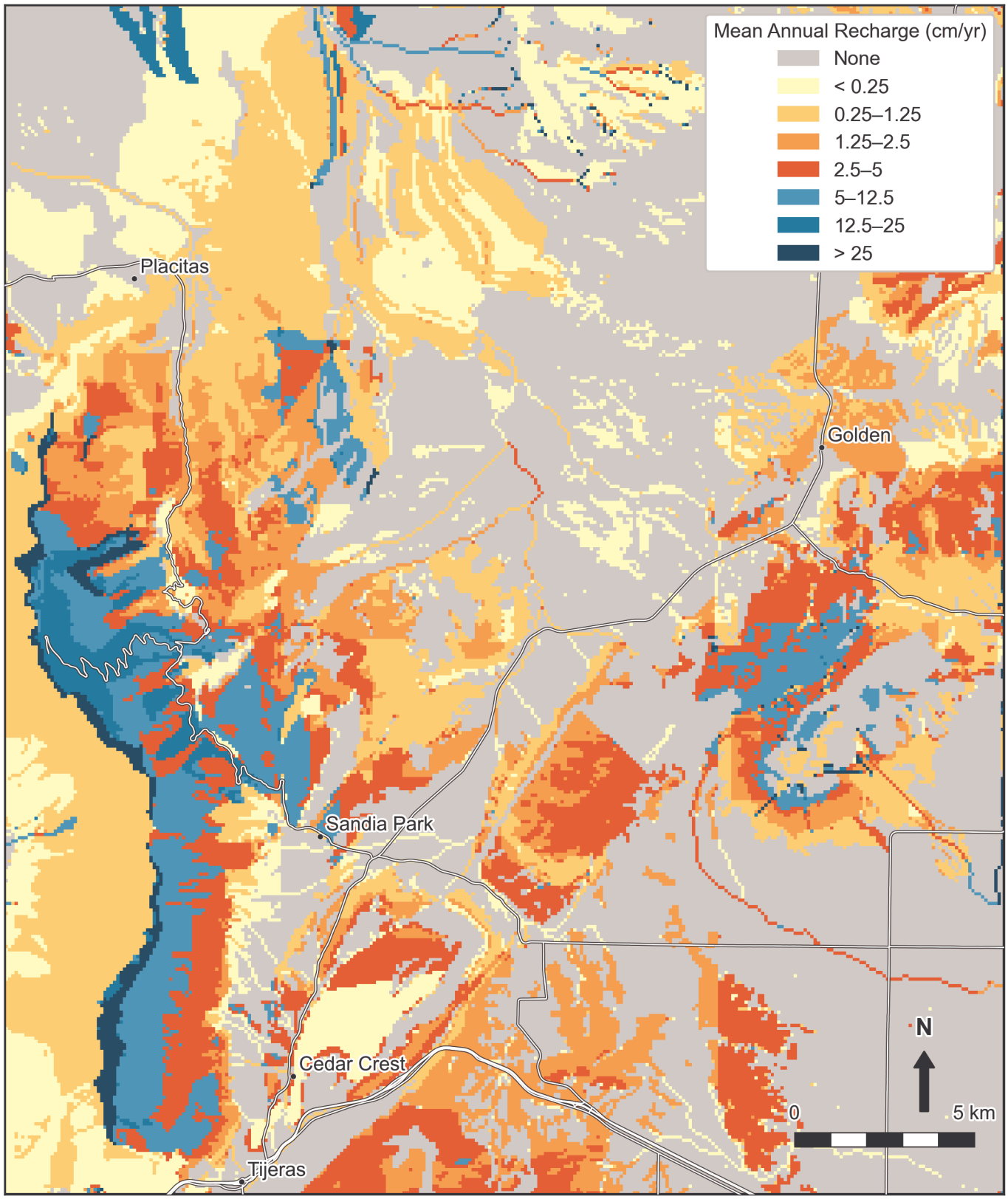


FIGURE 6. Map of mean annual recharge simulated by DPWM.

the chloride mass balance method, which uses chloride as a conservative tracer to estimate recharge rates from the ratio of chloride in bulk precipitation to chloride in groundwater, which is an approach well suited to arid and semiarid systems where recharge rates are low relative to precipitation (Rice and Crilley, 2014; Wilson and Guan, 2004). The chloride mass balance method thus provides an independent, tracer-based benchmark against which DPWM results can be compared. Insufficient spring discharge and baseflow measurements exist to compare to the DPWM recharge estimates.

The DPWM mean annual recharge estimate for the Madera Formation area above 2,286 m compares favorably with USGS estimates, though it falls below the USGS median. McCoy and Blanchard (2008) estimated recharge for the 34 km^2 area at 1.2 × 10^6 m^3/yr to 4.3 × 10^6 m^3/yr, representing 7% to 23% of mean annual precipitation, with a median of 2.8 × 10^6 m^3/yr. The DPWM estimated mean annual recharge of 2.2 × 10^6 m^3/yr for the same area, approximately 20% below the USGS median. Rice and Crilley (2014), whose study extended the McCoy and Blanchard (2008) area to include lower-elevation springs, estimated recharge ranging from 5.5% to 23% of annual precipitation. The DPWM estimated 4% of precipitation in the Madera area becomes recharge which falls near the lower end of this range.

Bartolino et al. (2010) estimated San Pedro Creek watershed recharge at 0.5 × 10^6 m^3/yr to 9.5 × 10^6 m^3/yr with a median of 5.0 × 10^6 m^3/yr. The DPWM estimated 4.1 × 10^6 m^3/yr for this same watershed area, representing 4% of simulated mean annual precipitation (104 × 10^6 m^3/yr) by DPWM. The DPWM recharge estimate is approximately 18% lower than the median estimate by Bartolino et al. (2010).

Douglas-Mankin et al. (2020) reported precipitation, actual evapotranspiration, and available water for calendar year 2015 in eastern Bernalillo County as 608 mm, 543 mm, and 65 mm, respectively, with available water (including runoff, recharge, and soil storage changes) representing approximately 11% of precipitation. For water year 2015 (slightly above average precipitation), the DPWM estimated spatially averaged precipitation of 446 mm, actual evapotranspiration of 359 mm, sublimation of 68 mm, and available water of 19 mm. Direct comparison is not appropriate because the SSEBop model estimates actual evapotranspiration from vegetated land surfaces using satellite thermal imagery and does not account for snow sublimation as a separate water loss. In the DPWM, sublimation represents approximately 15% of precipitation for water year 2015; excluding this term from total losses raises DPWM available water to approximately 20% of precipitation, indicating that the difference between the two studies is largely attributable to this accounting difference between the methods.

CONCLUSIONS

Local recharge from precipitation is the dominant input to the East Mountains groundwater system; lateral groundwater inflows from adjacent basins are considered negligible within the study domain (Bartolino et al., 2010). The DPWM provides a detailed and independent quantification of groundwater recharge for the East Mountains region of New Mexico. The fine spatial discretization of over 110,000 grid cells and a daily water mass balance spanning 45 years (1971–2015) assimilates data on climate, topography, soils, and vegetation. The mean annual recharge across the study area is estimated at approximately 15 × 10^6 m^3/yr, which is about 4% of average

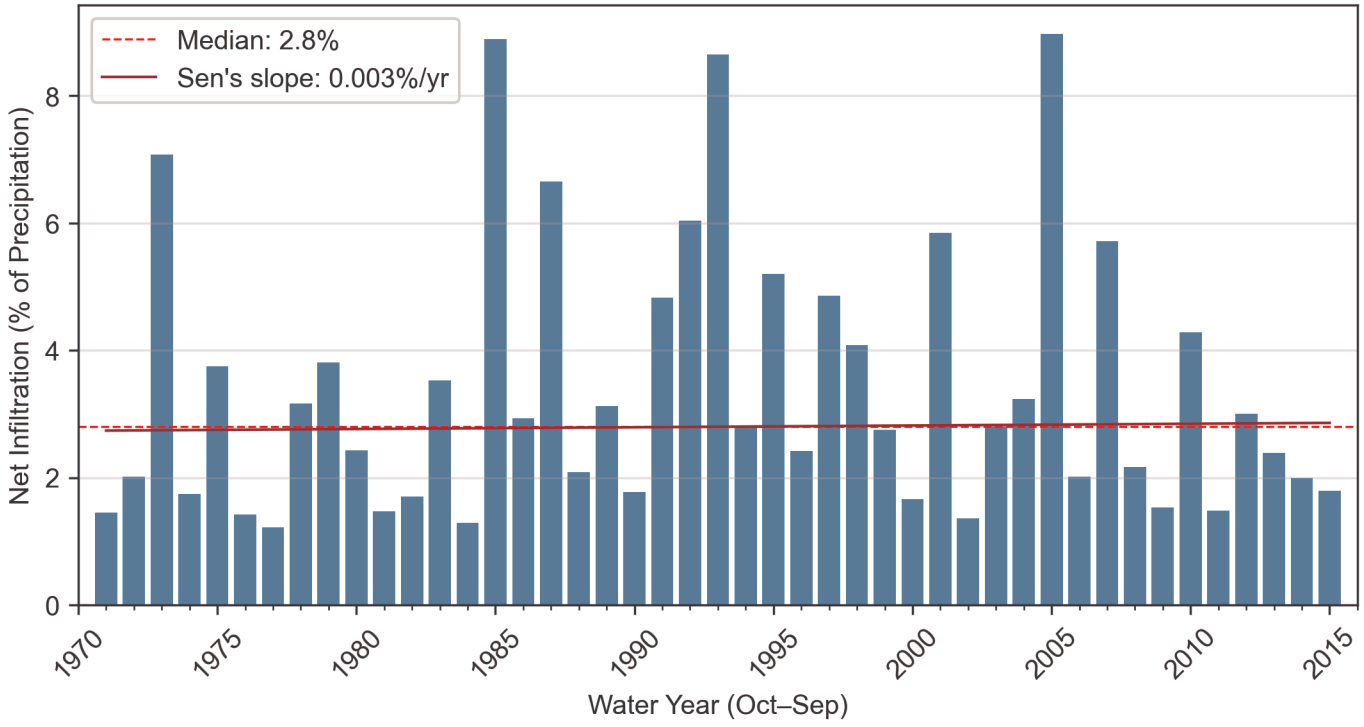


FIGURE 7. Plot of total annual recharge within the DPWM model domain for water years 1971 to 2015.

annual precipitation. The recharge is highly localized, occurring primarily at higher elevations in the Sandia Mountains and through focused infiltration along washes at lower elevations. Conversely, diffuse recharge between these washes was found to be negligible.

The recharge estimate obtained using the DPWM falls near the lower end of the range of recharge measurements and estimates published by the USGS. This lower estimate results from selecting parameter values that minimize recharge where model uncertainty exists; nearly 50% of the groundwater model area shows no recharge at all. The DPWM thus provides a lower bound estimate of recharge for the East Mountains area, which can be used to assess available groundwater resources for wells. Additionally, the model could be coupled with scaled climate models to predict groundwater recharge under future climate conditions.

REFERENCES

Allen, R.G., Pereira, L.S., Raes, D., and Smith, M., 1998, Crop evapotranspiration—Guidelines for computing crop water requirements: Food and Agriculture Organization of the United Nations (FAO) Irrigation and Drainage Paper 56, Rome, Italy, 300 p.

Allen, R.G., Trezza, R., and Tasumi, M., 2006, Analytical integrated functions for daily solar radiation on slopes: Agricultural and Forest Meteorology, v. 139, no. 1–2, p. 55–73. https://doi.org/10.1016/j.agrformet.2006.05.012

Bartolino, J.R., Anderholm, S.K., and Myers, N.C., 2010, Groundwater resources of the East Mountain area, Bernalillo, Sandoval, Santa Fe, and Torrance Counties, New Mexico, 2005: U.S. Geological Survey Scientific Investigations Report 2009-5204, 88 p. https://doi.org/10.3133/sir20095204

D'Agnese, F.A., Faunt, C.C., Turner, A.K., and Hill, M.C., 1997, Hydrogeologic evaluation and numerical simulation of the Death Valley regional ground-water flow system, Nevada and California: U.S. Geological Survey Water-Resources Investigations Report 96-4300, 124 p. https://doi.org/10.2172/573102

Daly, C., Neilson, R.P., and Phillips, D.L., 1994, A statistical-topographic model for mapping climatological precipitation over mountain terrain: Journal of Applied Meteorology and Climatology, v. 33, no. 2, p. 140–158. https://doi.org/10.1175/1520-0450(1994)033<0140:ASTMFM>2.0.CO;2

Daniel B. Stephens & Associates, Inc., 2009, Supplemental report: Distributed Parameter Watershed Model description, benchmarking, uncertainty and sensitivity analyses, and Maxey-Eakin method review for the Tule Desert Hydrographic Basin, Lincoln County, Nevada: Prepared for Lincoln County Water District and Vidler Water Company, 84p.

Douglas-Mankin, K.R., McCutcheon, R.J., Mitchell, A.C., and Senay, G.B., 2020, Landscape and climatic influences on actual evapotranspiration and available water using the Operational Simplified Surface Energy Balance (SSEBop) model in eastern Bernalillo County, New Mexico, 2015: U.S. Geological Survey Scientific Investigations Report 2020-5095, 40 p., https://doi.org/10.3133/sir20205095

Duffie, J.A., and Beckman, W.A., 1980, Solar Engineering of Thermal Processes, 1st edition: New York, John Wiley & Sons, 786 p.

Duffie, J.A., and Beckman, W.A., 1991, Solar Engineering of Thermal Processes, 2nd edition: New York, John Wiley & Sons, 942 p.

Flint, A.L., and Flint, L.E., 2007, Application of the Basin Characterization Model to estimate in-place recharge and runoff potential in the Basin and Range carbonate-rock aquifer system, White Pine County, Nevada, and adjacent areas in Nevada and Utah: U.S. Geological Survey Scientific Investigations Report 2007-5099, 21 p. https://doi.org/10.3133/sir20075099

Hevesi, J.A., Flint, A.L., and Flint, L.E., 2003, Simulation of net infiltration and potential recharge using a Distributed-Parameter Watershed Model of the Death Valley region, Nevada and California: U.S. Geological Survey Water-Resources Investigations Report 2003-4090, 162 p. https://doi.org/10.3133/wri034090

Julyan, R., and Steuver, M., eds., 2005, Field Guide to the Sandia Mountains: Albuquerque, University of New Mexico Press, 255 p.

Leavesley, G.H., Lichty, R.W., Troutman, B.M., and Saindon, L.G., 1983, Precipitation-runoff modeling system: User's manual: U.S. Geological Survey Water-Resources Investigations Report 83-4238, 207 p. https://doi.org/10.3133/wri834238

Lowry, J.H, Jr., Ramsey, R.D., Boykin, K., Bradford, D., Comer, P., Falzarano, S., Kepner, W., Kirby, J., Langs, L., Prior-Magee, J., Manis, G., O'Brien, L., Sajwaj, T., Thomas, K.A., Rieth, W., Schrader, S., Schrupp, D., Schulz, K., Thompson, B., Velasquez, C., Wallace, C., Waller, E., and Wolk. B., 2005, The Southwest Regional Gap Analysis Project: Final Report on Land Cover Mapping Methods: Logan, Utah State University, RS/GIS Laboratory, 50 p. https://rsgis-swregap.s3-us-west-2.amazonaws.com/public/docs/swregap_landcover_report.pdf

Maxey, G.B., and Eakin, T.E., 1949, Ground water in White River Valley, White Pine, Nye, and Lincoln Counties, Nevada: Nevada State Engineer Water Resources Bulletin 8, 121 p. http://images.water.nv.gov/images/publications/water%20resources%20bulletins/Bulletin8.pdf

McCoy, K.J., and Blanchard, P.J., 2008, Precipitation, ground-water hydrology, and recharge along the eastern slopes of the Sandia Mountains, Bernalillo County, New Mexico: U.S. Geological Survey Scientific Investigations Report 2008-5179, 34 p. https://doi.org/10.3133/sir20085179

Phillips, F.M., 1994, Environmental tracers for water movement in desert soils of the American Southwest: Soil Science Society of America Journal, v. 58, no. 1, p. 15–24. https://doi.org/10.2136/sssaj1994.03615995005800010003x

Reindl, D.T., Beckman, W.A., and Duffie, J.A., 1990, Diffuse fraction correlations: Solar Energy, v. 45, no. 1, p. 1–7. https://doi.org/10.1016/0038-092X(90)90060-P

Rice, S.E., and Crilley, D.M., 2014, Estimates of groundwater recharge rates and sources in the East Mountain area, eastern Bernalillo County, New Mexico, 2005–12: U.S. Geological Survey Scientific Investigations Report 2014-5181, 24 p. https://doi.org/10.3133/sir20145181

Schaap, M.G., Leij, F.J., and van Genuchten, M.T., 2001, ROSETTA: A computer program for estimating soil hydraulic parameters with hierarchical pedotransfer functions: Journal of Hydrology, v. 251, no. 3–4, p. 163–176. https://doi.org/10.1016/S0022-1694(01)00466-8

Schroeder, P.R., Dozier, T.S., Zappi, P.A., McEnroe, B.M., Sjostrom, J.W., and Peyton, R.L., 1994, The Hydrologic Evaluation of Landfill Performance (HELP) model: Engineering documentation for version 3: Washington, D.C., U.S. Environmental Protection Agency, Office of Research and Development, Risk Reduction Engineering Laboratory, EPA/600/R-94/168b, 116 p.

Soil Survey Staff, 2010, Soil survey geographic (SSURGO) database, for soil survey areas NM600, NM656, and NM687: U.S. Department of Agriculture, Natural Resources Conservation Service: https://websoilsurvey.sc.egov.usda.gov/app/WebSoilSurvey.aspx (accessed November 30, 2010).

Stein, J.S., Reed, A., Allen, R., Rasmuson, K., Kalinina, E., and Kanney, J., 2007, Simulation of net infiltration for present-day and potential future climates: Yucca Mountain Project, MDL-NBS-HS-000023 REV 01, prepared for U.S. Department of Energy by Sandia National Laboratories, Albuquerque, New Mexico, 942 p.

Stewart-Deaker, A.E., Stonestrom, D.A., and Moore, S.J., 2007, Streamflow, infiltration, and ground-water recharge at Abo Arroyo, New Mexico: U.S. Geological Survey Professional Paper 1703-D, 23 p. https://doi.org/10.3133/pp1703D

U.S. Geological Survey (USGS), 2008, Documentation of computer program INFIL3.0—A Distributed-Parameter Watershed Model to estimate net infiltration below the root zone: U.S. Geological Survey Scientific Investigations Report 2008-5006, 98 p. https://doi.org/10.3133/sir20085006

U.S. Geological Survey (USGS), 2010, MODIS datasets, accessed through Global Visualization Viewer, "MODIS Terra" collection and "MOD15A2 LAI" images: http://glovis.usgs.gov/ (accessed December 2010).

U.S. Geological Survey (USGS), 2026, Gap analysis project: https://www.usgs.gov/programs/gap-analysis-project (accessed 2011).

Williams, P.L., and Cole, J.C., 2007, Geologic map of the Albuquerque 30' x 60' quadrangle, north-central New Mexico: U.S. Geological Survey Scientific Investigations Map 2946, 31 p. https://doi.org/10.3133/sim2946

Wilson, J.L., and Guan, H., 2004, Mountain-block hydrology and mountain-front recharge, *in* Hogan, J.F., Philips, F.M., and Scanlon, B.R., eds., Groundwater recharge in a desert environment: The southwestern United States: American Geophysical Union Water Science and Applications Series, v. 9, p. 113–137. https://doi.org/10.1029/009WSA08